Scholars Bulletin *(Engineering & Technology)*

An Official Publication of "Scholars Middle East Publishers", Dubai, United Arab Emirates
Website: http://scholarsbulletin.com/

ISSN 2412-9771 (Print)
ISSN 2412-897X (Online)

Influence of Suitable Admissible Functions for the Lateral Displacement in Thermal Post-Buckling Response of Orthotropic Circular Plates

Anju V Nair[1], Sharidan Shafie[2], Abdul Rahman, Mohd Kasim[1], Mohd Zuki Salleh[1]

[1]Faculty of Industrial Sciences & Technology, Universiti Malaysia Pahang, Lebuhraya Tun Razak, 26300, Gambang, Kuantan, Malaysia

[2]Departments of Mathematical Sciences, Universiti Teknologi Malaysia, 81310 Johor Bahru, Johor, Malaysia

***Corresponding author**
Abdul Rahman Mohd Kasim

Article History
Received: 06.12.2017
Accepted: 12.12.2017
Published: 30.12.2017

DOI:
10.21276/sb.2017.3.12.7

Abstract: An accurate formulation to predict the thermal post-buckling load carrying capacity of orthotropic circular plates based on von Kàrmàn nonlinearities is reported in this paper. The governing differential equations of circular plates with orthotropic material properties are converted into linear differential equations employing the nondimensional parameters. The radial edge load is evaluated by assuming suitable admissible functions for the lateral displacement. Simply supported and clamped boundary conditions are considered in this study. The Rayleigh - Ritz method of total potential energy gives the values of linear buckling load. The thermal postbuckling load of orthotropic circular plates is evaluated using the radial edge load and linear buckling load. The influences of suitable admissible functions on the lateral displacement are also discussed. The numerical results obtained from the present investigation are compared with the known results reported in the literature and are in good agreement within the engineering accuracy. The error percentage of the results has been predicted and a maximum error is found out to be 4.02 % for simply supported and 3.67 % for clamped boundary conditions respectively.

Keywords: Orthotropic circular plate; Thermal post-buckling; Radial edge tensile load; von Kàrmàn nonlinearity.

Nomenclature

a = radius of the circular plate
N_r = uniform radial edge compressive load per unit length
$N_{r_{cr}}$ = linear buckling load
$N_{r_{NL}}$ = total uniform radial edge compressive load per unit length
N_{r_T} = uniform radial edge tensile load per unit length developed due to large lateral displacements
h = thickness of the plate
ΔT = temperature rise from the stress free temperature
$\varepsilon_r, \varepsilon_\theta$ = in – plane strains
ν_r, ν_θ = Poisson's ratio
U = strain energy
r, θ = radial and circumferential coordinates
W = work done
χ_r, χ_θ = curvatures
r_1, r_2 = internal and external radii
$\alpha_1 - \alpha_6$ = generalized displacements
β = orthotropic parameter
E_r, E_θ = Young's moduli in radial and circumferential directions
γ = postbuckling load
b_0 = central (maximum) lateral displacement of the circular plate

INTRODUCTION

Circular plates are common structural members used in the analysis of structures in different fields of engineering such as mechanical, automobile, manufacturing, civil, marine and aerospace systems. With the present day, highly optimum and cost effective designs in structural engineering, it is not necessary to treat that the structure fails at the buckling load, contrary to the popular belief. The inherent geometric nonlinearity involved gives an additional load carrying capacity to the structures after phenomenon of buckling [1, 2]. The structures are capable of taking additional compressive loads with high deformations. But, if these deformations are tolerable and do not affect the functional requirements, the additional load carrying capacity of these structure, called as the post-buckling load, can be advantageously used in the design process. Further, the thermal post-buckling load, due to a temperature rise from the stress free temperature, in the service condition of these structures, is an order of higher in magnitude than the mechanical loads as seen in the literature [1, 2]. This property can be used advantageously for aerospace and other structures subjected to thermal loads due to the temperature raise. In order to obtain, the effective response of these structural members, prediction of the thermal post-buckling load of these plates is essential. The evaluation of radial edge tensile load parameter becomes tedious because of the coupling between the radial and the circumferential strain components. Hence, some approximations have to be assorted to evaluate the radial edge tensile load of the circular plate.

The postbuckling behavior of circular plates has been studied by many researchers. The post-buckling behavior of cylindrically orthotropic circular plates through the finite element formulation has been presented by Raju and Rao [3]. In the books of Thompson and Hunt [1] and Dym [2] investigated the post-buckling behavior of uniform, isotropic circular and rectangular plates under mechanical loads analytically. Finite element formulation and Rayleigh–Ritz analysis to obtain the thermal post-buckling behavior of isotropic plates and comparison of the numerical results has been presented by Raju and Rao [4]. Rao and Varma [5], offered a simple formulation to predict the thermal post-buckling load of circular plates and the method of evaluating the radial edge tensile load developed due to the large lateral displacement. The thermal post-buckling analysis of tapered columns and uniform columns with immovable ends in the axial direction is reported by [6, 7]. Moreover, the thermal post-buckling of circular plates using Berger's approximation [8, 9] are presented.

Based on von Kàrmàn's nonlinear plate theory, the effects of material properties and non-uniform temperature rise parameters on the axisymmetric thermal post-buckling behavior of functionally graded material circular plates under immovably clamped boundary and a transversely point space constraints has been investigated by Sun and Li [10]. Axisymmetric large deflection bending and thermal post-buckling behavior of functionally graded circular plate subjected to thermal, mechanical and combined thermal–mechanical loadings using the classical von Kàrmàn plate theory has been studied by Ma and Wang [11, 12]. The effects of material properties and boundary conditions on the nonlinear bending and thermal postbuckling behavior of functionally graded plates are considered and shooting method is used to solve numerically the governing equations. Further, thermal buckling of circular plates made of functionally graded materials has been investigated by Najafizadeh and Eslami [13, 14] by deriving the nonlinear equilibrium and linear stability equations using variational methods. In this study, uniform temperature rise and thermal gradient through the thickness are considered and their thermal postbuckling loads are evaluated.

The axisymmetric vibrations of thermally post buckled circular plates with uniform temperature rise has been studied by Li *et.al* [15]. The effects of geometric boundary conditions with simply supported and clamped boundary conditions are considered in this study. Raju and Rao [16] used a general finite element formulation to disclose the effects of plate thickness and tapered parameter on the thermal post-buckling behavior of linearly tapered moderately thick isotropic circular plates under thermal loads. A modified Berger's approximation to study the large amplitude vibration behavior of circular plates has been discussed by Rao *et al.* [17]. In their studies, the radial tension T is evaluated using suitable assumptions, based on von Kàrmàn nonlinear strain – displacement relations and the results are presented in terms of the square of the ratios of the nonlinear to the linear angular frequencies.

Finite element formulation approach for the post-buckling behavior of tapered circular plates with cylindrically orthotropic material properties for different values of the taper parameter and orthotropic parameter with simply supported and clamped boundary conditions has been discussed in [18]. A study has been carried out on the post-buckling behavior of cylindrically orthotropic plates on elastic foundation with edges elastically restrained against rotation in [19]. The numerical results of linear buckling load parameters and radial load ratios for various values of orthotropic parameters have been reported. The post-buckling behavior of moderately thick circular plates with cylindrically orthotropic material properties has been mentioned in [20] by using finite element formulation approach. In

all these studies, these methods take more computational efforts to obtain the approximate solutions because of the nonlinear nature of the problem.

The aim of this paper is to present a new numerical approach to attain the thermal post-buckling load of orthotropic circular plates using approximations based on von Kármán nonlinearities. The advantage of the present formulation is that it needs only the knowledge of linear buckling load and uniform radial edge tensile load developed due to the lateral displacement, '*w*'.

In the following section, the evaluation of radial edge tensile load, linear buckling load parameters and hence thermal post-buckling load carrying capacity, by assuming suitable functions for the lateral displacement '*w*' are described. The effects of three approximate functions are analyzed to obtain the radial edge tensile load developed in the circular plate. Both simply supported and clamped boundary conditions of the circular plate are considered in this study and the numerical results are obtained by taking the value of Poisson's ratio as 0.3. Furthermore, the results obtained from the present investigation are compared with the previous results evaluated using finite element method [3].

Mathematical formulation

A circular plate of radius *'a'* and of uniform thickness *'h'* under a uniform compressive radial load 'N_r' per unit length at the boundary is illustrated in Figure 1.

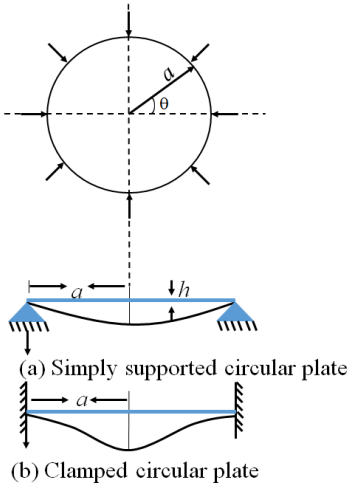

Fig-1: A circular plate showing coordinate system and lateral deflection pattern with both boundary conditions

If the plate is heated to a temperature ΔT from the stress free state, an equivalent uniform compressive radial edge load N_r will be developed in the plate. This ΔT can transform to the critical temperature (ΔT_r) on further heating and develops critical compressive radial edge load $N_{r_{cr}}$ resulting in plate buckling. Further increase in ΔT induces large lateral displacements of the plate resulting in the development of uniform tensile edge load N_{r_T}. This N_{r_T}, for a central (maximum) lateral displacement, permits the plate to withstand more N_r beyond N_{cr}. Therefore, the total equivalent compressive uniform radial edge load carrying capacity of the circular plate $\left(N_{r_{NL}}\right)$, namely postbuckling load, will be mathematically represented as

$$\overline{N}_{r_{NL}} = \overline{N}_{r_{cr}} + \overline{N}_{r_T} \tag{1}$$

$$N_{r_{NL}} = N_{r_T} + N_{r_{cr}} \tag{2}$$

or in the non-dimensional form as

$$\frac{\overline{N}_{r_{NL}}}{\overline{N}_{r_{cr}}} = 1 + \frac{\overline{N}_{r_T}}{\overline{N}_{r_{cr}}} \tag{3}$$

where the term $\overline{N}_{r_T}$ in equation (3) is non – dimensionalized as

$$\overline{N}_{r_T} = \frac{N_r a^2}{D} \tag{4}$$

in which D is the plate flexural rigidity $D = \frac{E h^3}{12\left(1-\nu^2\right)}$. The thermal load equivalent of N_r is given by

$$\overline{N}_r = \frac{\alpha E_\theta h}{1-\nu_r \nu_\theta} \tag{5}$$

(a) Evaluation of radial edge tensile load due to large lateral displacements

The uniform radial edge tensile load developed in the circular plate with radially immovable edges is calculated using the following procedure.

After relaxing the static conditions at the circular plate's edge, a large axisymmetric lateral displacement is provided at its edge. An inward radial edge displacement will be developed in its edge owing to it. A uniform radial tensile load is applied on the edge of the plate for compensating this inward radial displacement resulting an outward radial edge displacement. The condition for determining the magnitude of uniform radial edge tensile load is that the magnitudes of the inward radial edge displacement due to large axisymmetric lateral displacement and the outward radial edge displacement due to the applied uniform radial edge tensile load are equal. The inward and outward radial edge displacement expressions are derived in this section.

The von Kàrmàn nonlinear strain-displacement relations of the circular plate for large lateral axisymmetric displacements are [3]

$$\varepsilon_r = \frac{du}{dr} + \frac{1}{2}\left(\frac{dw}{dr}\right)^2 \tag{6}$$

$$\varepsilon_\theta = \frac{u}{r} \tag{7}$$

$$\chi_r = -\frac{d^2 w}{dr^2} \tag{8}$$

$$\chi_\theta = -\frac{1}{r}\left(\frac{dw}{dr}\right) \tag{9}$$

Where r and θ are the radial and circumferential coordinates, $\varepsilon_r, \varepsilon_\theta$ are the strains and χ_r, χ_θ are the curvatures.

Because of the expansion of the laterally deformed surface of the circular plate, the expression for N_r can be written from equations (6) and (7) as

$$N_r = \frac{E_\theta h}{\beta - \nu_\theta^2}\left[\varepsilon_r + \nu_\theta \varepsilon_\theta\right] \tag{10}$$

$$\text{Or } N_r = \frac{E_\theta h}{\beta - \nu_\theta^2}\left[\frac{du}{dr} + \frac{1}{2}\left(\frac{dw}{dr}\right)^2 + \nu_\theta \frac{u}{r}\right] \tag{11}$$

$$\text{And } N_\theta = \frac{E_\theta h}{\beta - \nu_r \nu_\theta}\left[\nu_\theta\left(\frac{du}{dr} + \frac{1}{2}\left(\frac{dw}{dr}\right)^2\right) + \beta.\frac{u}{r}\right] \tag{12}$$

According to Berger's approximation [21], the second invariant of the strains are neglected or $\varepsilon_r << \varepsilon_\theta$, N_r can be written as

$$N_r = \frac{E_\theta h}{\beta - \nu_\theta^2}\left[\frac{du}{dr} + \frac{1}{2}\left(\frac{dw}{dr}\right)^2\right] \tag{13}$$

$$\text{And } N_\theta = \frac{E_\theta h}{\beta - \nu_r \nu_\theta}\left[\nu_\theta\left(\frac{du}{dr} + \frac{1}{2}\left(\frac{dw}{dr}\right)^2\right)\right] \tag{14}$$

In equations (13) and (14), $N_r = 0$ and $N_\theta = 0$ give the relation for the inward radial edge displacement as

$$u_I = -\frac{1}{2}\int_0^a \left(\frac{dw}{dr}\right)^2 dr \tag{15}$$

By considering the sector of the plate with a subtended angle θ at the centre, the outward radial edge displacement u_T can be calculated. Therefore,

$$u_T = \frac{N_{rT} a}{E_\theta h} \tag{16}$$

Since the magnitudes of u_I and u_T are equal, it gives the radial edge tensile load N_{rT} and can be expressed as

$$N_{r_T} = \frac{E_\theta h}{2a}\int_0^a \left(\frac{dw}{dr}\right)^2 dr \tag{17}$$

Hence the uniform radial edge tensile load developed in the circular plate due to large deflections can be obtained in the non – dimensional form as

$$N_{r_T} = \frac{6a\left(\beta - \nu_r \nu_\theta\right)}{\left(h^2\right)}\int_0^a \left(\frac{dw}{dr}\right)^2 dr \tag{18}$$

For simply supported immovable edges, $u = 0$ but $\frac{dw}{dr} \neq 0$ and for clamped edge, $u = 0$ and $\frac{dw}{dr} = 0$ is used to evaluate the numerical results.

(b) Evaluation of linear buckling load and postbuckling load carrying capacity

Considering the strain – displacement relations from (6) to (9) , the strain energy U of the plate with orthotropic material properties [3], is given by

$$U = \frac{1}{2}\int_0^{2\pi}\int_{r_1}^{r_2}\left[C_1\varepsilon_r^{\,2} + C_2\,\varepsilon_\theta^{\,2} + C_{12}\,\varepsilon_r\varepsilon_\theta + D_1\,\chi_r^{\,2} + D_2\,\chi_\theta^{\,2} + D_{12}\,\chi_r\chi_\theta\right] r\,dr\,d\theta \tag{19}$$

where $C_1 = \frac{E_r h}{1-\nu^2}$, $C_2 = \frac{E_\theta h}{1-\nu^2}$, $C_{12} = \nu_r C_2 = \nu_\theta C_1$, $D_1 = \frac{E_r h^3}{12\left(1-\nu^2\right)}$, $D_2 = \frac{E_\theta h^3}{12\left(1-\nu^2\right)}$, and $D_{12} = \nu_r D_2 = \nu_\theta D_1$.

Substituting the values of C1, C_2, C_{12}, D_1, D_2, D_{12}, and using equations (6) to (9) in equation (19), it can be written as

$$\begin{aligned} U = \frac{1}{2}\int_0^{2\pi}\int_{r_1}^{r_2} & \frac{E_r h}{1-\nu_r\nu_\theta}\left(\frac{du}{dr}+\frac{1}{2}\left(\frac{dw}{dr}\right)^2\right)^2 + \frac{E_\theta h}{1-\nu_r\nu_\theta}\left(\frac{u}{r}\right)^2 \\ & + \nu_r\cdot\frac{E_\theta h}{1-\nu^2}\cdot\left(\frac{du}{dr}+\frac{1}{2}\left(\frac{dw}{dr}\right)^2\right)\cdot\left(\frac{u}{r}\right) + \frac{E_r h^3}{12\left(1-\nu_r\nu_\theta\right)}\left(-\frac{d^2w}{dr^2}\right)^2 \\ & + \frac{E_\theta h^3}{12\left(1-\nu_r\nu_\theta\right)}\left(-\frac{1}{r}\cdot\frac{dw}{dr}\right)^2 + \nu_r\frac{E_\theta h^3}{12\left(1-\nu_r\nu_\theta\right)}\cdot\left(-\frac{d^2w}{dr^2}\right)\cdot\left(-\frac{1}{r}\cdot\frac{dw}{dr}\right) r\,dr\,d\theta \end{aligned} \tag{20}$$

$$\begin{aligned} U = \frac{1}{2}\frac{E_r h}{1-\nu_r\nu_\theta}\int_0^1 & \left(\frac{du}{dr}\right)^2 + \left(\frac{du}{dr}\cdot\left(\frac{dw}{dr}\right)^2\right) + \left(\frac{1}{2}\left(\frac{dw}{dr}\right)^2\right)^2 + \frac{E_\theta}{E_r}\left(\frac{u}{r}\right)^2 \\ & + \nu_r\cdot\frac{E_\theta}{E_r}\cdot\left(\frac{du}{dr}+\frac{1}{2}\left(\frac{dw}{dr}\right)^2\right)\cdot\left(\frac{u}{r}\right) + \frac{h^2}{12}\left(\frac{d^2w}{dr^2}\right)^2 \\ & + \frac{E_\theta h^2}{12E_r}\left(\frac{1}{r}\cdot\frac{dw}{dr}\right)^2 + \nu_r\frac{E_\theta h^2}{12E_r}\cdot\left(\frac{d^2w}{dr^2}\right)\cdot\left(\frac{1}{r}\cdot\frac{dw}{dr}\right) r\,dr \end{aligned} \tag{21}$$

By referring [22], the integral becomes,

$$U = \frac{1}{2}\int_0^1 \left[\begin{array}{l} \frac{1}{4}\left(\frac{dw}{dr}\right)^4 + \frac{h^2}{12}\left(\frac{d^2w}{dr^2}\right)^2 + \left(\frac{E_\theta}{E_r}\right).\frac{h^2}{12}.\frac{1}{r^2}.\left(\frac{dw}{dr}\right)^2 \\ \qquad + \nu.\left(\frac{E_\theta}{E_r}\right).\frac{h^2}{12}.\frac{1}{r}.\left(\frac{d^2w}{dr^2}\right).\left(\frac{dw}{dr}\right) \end{array} \right] r\,dr \tag{22}$$

Eliminating *h* from equation (22), we can write the reduced equation for strain energy as

$$U = \frac{1}{2}\int_0^1 \left[\left(\frac{d^2w}{dr^2}\right)^2 + \left(\frac{\beta}{r^2} - \frac{\beta^2}{4}\right)\left(\frac{dw}{dr}\right)^2 + \frac{\nu\beta}{r}\left(\frac{d^2w}{dr^2}\right)\left(\frac{dw}{dr}\right) \right] r\,dr \tag{23}$$

Where $\beta = E_\theta / E_r$ be the orthotropic parameter ($E_\theta \neq E_r$).

The work done, *W* by the external load N_r per unit length at the boundary of the element is given by [23]

$$W = \frac{1}{2}\int_0^{2\pi}\int_{r_1}^{r_2} \bar{N}_r \left(\frac{dw}{dr}\right)^2 r\,dr\,d\theta \tag{24}$$

Equation (24) can be written in the equivalent form of N_r as

$$W = \frac{\lambda}{2}\int_0^1 N_r \left(\frac{dw}{dr}\right)^2 r\,dr \tag{25}$$

By giving substitution for N_r given in equation (13), the expression for *W* can be written as

$$W = \frac{\lambda}{2}\int_0^1 \frac{E_\theta h}{1-\nu^2}\left(\frac{du}{dr} + \frac{1}{2}\left(\frac{dw}{dr}\right)^2\right)\left(\frac{dw}{dr}\right)^2 r\,dr \tag{26}$$

Eliminating *h* from the above equation, the simplified equation can be written as

$$W = \frac{\lambda\beta^3}{4}\int_0^1 \left(\frac{dw}{dr}\right)^2 r\,dr \tag{27}$$

The total potential energy of the plate can be stated as

$$\Pi = U - W \tag{28}$$

The total potential energy is the function of in – plane displacement fields and lateral displacement fields. Rayleigh – Ritz method [24-26] includes the minimization of the total potential energy with respect to the undetermined coefficients of the assumed admissible displacement functions.

In the present formulation, three different admissible functions for the lateral displacement '*w*', which satisfies the geometric boundary conditions, are assumed and the uniform radial edge tensile load N_{r_T} is evaluated using equation (18). Both simply supported and clamped boundary conditions are considered in this study.

The following admissible functions F_1, F_2, and F_3 for the lateral displacement '*w*' are used.

$$F_1 = b_0 \left(1 - \left(\frac{r}{a} \right)^2 \right)^n \tag{29}$$

$$F_2 = b_0 \cos^n \left(\frac{\pi r}{2a} \right) \tag{30}$$

$$F_3 = b_0 \left[1 + \alpha_1 \left(\frac{r}{a} \right)^2 + \alpha_2 \left(\frac{r}{a} \right)^4 \right] + b_1 \left[\alpha_3 \left(\frac{r}{a} \right)^2 + \alpha_4 \left(\frac{r}{a} \right)^4 + \left(\frac{r}{a} \right)^6 \right] + b_2 \left[\alpha_5 \left(\frac{r}{a} \right)^4 + \alpha_6 \left(\frac{r}{a} \right)^6 + \left(\frac{r}{a} \right)^8 \right] \tag{31}$$

The functions satisfy the following boundary conditions.

(i) *Simply supported:* At $r = 0$, $w' = 0$; At $r = a$, $w = 0$

(ii) *Clamped:* At $r = 0$, $w' = 0$; At $r = a$, $w = 0$, $w' = 0$.

Equations (29) and (30), the simple algebraic and trigonometric functions, satisfy the geometric boundary conditions whereas equation (31), taken from [27] satisfies both geometric and natural boundary conditions. The values of $n = 1$ and $n = 2$ represent the simply supported and clamped boundary conditions, for the functions F_1 and F_2 respectively. In equation (31), the coefficients b_0, b_1 and b_2 of the first and second terms are normalized with the coefficient of the first term b_0. For clamped circular plates, the values of α_1, α_2, α_3, α_4, α_5 and α_6 are –2, 1, 1, –2, 1, –2 respectively. For simply supported circular plates, the values of α_1, α_2, α_3, α_4, α_5 and α_6, are given in terms of ν and β as [28]

$$\alpha_1 = -\frac{12 + 4\nu + 4\beta}{10 + 2\nu + 2\beta}, \quad \alpha_2 = \frac{2 + 2\nu + 2\beta}{10 + 2\nu + 2\beta}, \quad \alpha_3 = \frac{18 + 2\nu + 2\beta}{10 + 2\nu + 2\beta}, \quad \alpha_4 = -\frac{28 + 4\nu + 4\beta}{10 + 2\nu + 2\beta}$$

$$\alpha_5 = \frac{26 + 2\nu + 2\beta}{18 + 2\nu + 2\beta}, \text{ and } \alpha_6 = -\frac{44 + 4\nu + 4\beta}{18 + 2\nu + 2\beta} \tag{32}$$

for the function F_3.

The values of linear buckling load parameters $\bar{N}_{r_{cr}}$ (λ) can be evaluated by solving equation (28) with appropriate boundary conditions and by extracting the eigen values using MAPLE software. Substituting the displacement distributions and evaluating the integrations involved in equations (23) and (27), the Rayleigh – Ritz method of minimum total potential energy is given by $\frac{d\Pi}{db_0} = 0$ gives the system of solutions.

The ratio of the radial edge tensile load to the linear buckling load parameters, which represent the postbuckling load carrying capacity (γ), obtained from equation (2) can be written as

$$\gamma = \frac{N_{r_{NL}}}{N_{r_{cr}}} = 1 + c\left(\frac{b_0}{h}\right)^2 \tag{33}$$

The postbuckling behavior of the orthotropic circular plates can be obtained once the values of $\overline{N}_{r_T}$ and $\overline{N}_{r_{cr}}$ are known. The values of *c* for the functions F_1, F_2 and F_3 for simply supported plates are 1.7430, 1.6044, and 1.5967 as well as for the clamped circular plates are 0.4533, 0.4587 and 0.4533 respectively. The values of γ are evaluated for different values of the orthotropic parameter β ranging from 1.2 to 2.0 with varying values of b_0/h .

NUMERICAL RESULTS AND DISCUSSIONS

The radial edge tensile load and thermal post-buckling load carrying capacity of orthotropic circular plates is developed by assuming appropriate admissible functions for the lateral displacement '*w*' is presented in the research work. The admissible functions satisfy both simply supported and clamped boundary conditions. The radial edge tensile load and thermal post-buckling load for different β values ranging from 1.2 to 2.0 in steps of 0.2 are evaluated.

The thermal post buckling load values of simply supported and clamped orthotropic circular plates for several values of b_0/h using F_2 and F_3 are given in Tables (1 - 4). The postbuckling load evaluated using F_1 can be obtained from the published literature [29]. The numerical results obtained from the present investigation are compared with the results from reference [3] for different β values. It can be seen from the tables that the results from the present investigation are in good agreement with those obtained using finite element method. The highest error percentage from the reference is 4.02% for simply supported and 3.67% for clamped boundary conditions. It is assumed in the Berger's approximation that the strain energy due to the second variant of the middle surface strains can be neglected could be the reason for the much higher values for the simply supported and clamped circular plates.

Tables 1 - 2 represent the values of thermal post-buckling load carrying capacity (γ) for the assumed functions F_2 and F_3 respectively with simply supported boundary conditions. The error percentage obtained by comparing the present and previous numerical results is also included. The maximum percentage error obtained for the three assumed functions are less than 5% and are within the engineering accuracy. Moreover, it is noted that F_1 gives consistently better results for simply supported boundary conditions.

Table-2: Representing post-buckling load (γ) values of simply supported orthotropic circular plates for the assumed function $F_2 = b_0 \cos^n\left(\frac{\pi r}{2a}\right)$. '*' indicates the reference values taken from [3].

b_0/h	Present results									
	β = 1.2	Error (%)	β = 1.4	Error (%)	β = 1.6	Error (%)	β = 1.8	Error (%)	β = 2.0	Error (%)
0.0	2.2737 (2.2557)*	0.79	2.2623 (2.2466)*	0.7	2.2539 (2.2381)*	0.71	2.2386 (2.2300)*	0.39	2.2317 (2.2224)*	0.42
0.2	2.2966 (2.2661)*	1.34	2.2853 (2.2566)*	1.27	2.2731 (2.2478)*	1.12	2.2523 (2.2393)*	0.58	2.2433 (2.2314)*	0.53
0.4	2.3435 (2.2972)*	2.02	2.3212 (2.2866)*	1.51	2.3032 (2.2767)*	1.17	2.2847 (2.2673)*	0.77	2.2745 (2.2584)*	0.71
0.6	2.3994 (2.3487)*	2.16	2.3756 (2.3363)*	1.68	2.3571 (2.3246)*	1.40	2.3332 (2.3136)*	0.85	2.3170 (2.3032)*	0.60
0.8	2.4719 (2.4203)*	2.13	2.4443 (2.4054)*	1.62	2.4302 (2.3913)*	1.63	2.4096 (2.3780)*	1.33	2.3909 (2.3654)*	1.08
1.0	2.5541 (2.5114)*	1.7	2.5272 (2.4932)*	1.36	2.5063 (2.4761)*	1.22	2.4963 (2.4600)*	1.48	2.4791 (2.4448)*	1.40

Table-2: Representing postbuckling load (γ) values of simply supported orthotropic circular plates for the assumed function

$$F_3 = b_0\left[1+\alpha_1\left(\frac{r}{a}\right)^2+\alpha_2\left(\frac{r}{a}\right)^4\right]+b_1\left[\alpha_3\left(\frac{r}{a}\right)^2+\alpha_4\left(\frac{r}{a}\right)^4+\left(\frac{r}{a}\right)^6\right]+b_2\left[\alpha_5\left(\frac{r}{a}\right)^4+\alpha_6\left(\frac{r}{a}\right)^6+\left(\frac{r}{a}\right)^8\right]$$. '*' indicates the reference values taken from [3].

b_0/h	Present results									
	β = 1.2	Error (%)	β = 1.4	Error (%)	β = 1.6	Error (%)	β = 1.8	Error (%)	β = 2.0	Error (%)
0.0	2.2875 (2.2557)*	1.41	2.2723 (2.2466)*	1.32	2.2702 (2.2381)*	1.43	2.2608 (2.2300)*	1.38	2.2548 (2.2224)*	1.46
0.2	2.3189 (2.2661)*	2.33	2.3085 (2.2566)*	2.29	2.2921 (2.2478)*	1.97	2.2808 (2.2393)*	1.85	2.2719 (2.2314)*	1.81
0.4	2.3741 (2.2972)*	3.35	2.3577 (2.2866)*	3.11	2.3391 (2.2767)*	2.74	2.3218 (2.2673)*	2.41	2.3057 (2.2584)*	2.09
0.6	2.4431 (2.3487)*	4.02	2.4219 (2.3363)*	3.66	2.3967 (2.3246)*	3.10	2.3802 (2.3136)*	2.88	2.3635 (2.3032)*	2.62
0.8	2.5082 (2.4203)*	3.63	2.4895 (2.4054)*	3.49	2.4656 (2.3913)*	3.11	2.4446 (2.3780)*	2.80	2.4249 (2.3654)*	2.51
1.0	2.5707 (2.5114)*	2.36	2.5504 (2.4932)*	2.29	2.5282 (2.4761)*	2.10	2.5068 (2.4600)*	1.90	2.4854 (2.4448)*	1.66

Similarly, Tables 3 - 4 represent the values of γ and their error percentage from reference for the three admissible functions in the case of clamped orthotropic circular plates. As in the case of simply supported plates, the error percentage obtained with clamped boundary conditions are also less than 5% for the three assumed functions, within the engineering accuracy. Besides, it can be seen that the error percentage of clamped orthotropic circular plates are less than simply supported orthotropic circular plates. Furthermore, these three admissible functions give more or less the same values of γ for clamped orthotropic circular plates due to the edge boundary conditions of the plate. These results shows that one has to be careful in selecting admissible functions for simplifying nonlinear differential equations of the plates where geometric nonlinearity is involved to obtain accurate numerical results.

Table-3: Representing postbuckling load (γ) of clamped circular plates for the assumed function

$$F_2 = b_0\cos^n\left(\frac{\pi r}{2a}\right)$$. **'*' indicates the reference values taken from [3].**

b_0/h	Present results									
	β = 1.2	Error (%)	β = 1.4	Error (%)	β = 1.6	Error (%)	β = 1.8	Error (%)	β = 2.0	Error (%)
0.0	2.2266 (2.1951)*	1.44	2.2186 (2.1924)*	1.19	2.2143 (2.1894)*	1.14	2.2071 (2.1860)*	0.97	2.1996 (2.1824)*	0.79
0.2	2.2472 (2.2031)*	2.00	2.2354 (2.2003)*	1.59	2.2298 (2.1972)*	1.49	2.2247 (2.1936)*	1.42	2.2173 (2.1899)*	1.25
0.4	2.2796 (2.2271)*	2.36	2.2719 (2.2239)*	2.16	2.2653 (2.2204)*	2.02	2.2572 (2.2164)*	1.84	2.2461 (2.2122)*	1.53
0.6	2.3317 (2.2666)*	2.87	2.3239 (2.2629)*	2.69	2.3126 (2.2587)*	2.39	2.3093 (2.2540)*	2.45	2.2964 (2.2491)*	2.10
0.8	2.3928 (2.3212)*	3.08	2.3819 (2.3167)*	2.81	2.3757 (2.3117)*	2.77	2.3636 (2.3061)*	2.49	2.3516 (2.3002)*	2.24
1.0	2.4515 (2.3902)*	2.57	2.4428 (2.3848)*	2.43	2.4361 (2.3788)*	2.41	2.4253 (2.3720)*	2.25	2.4087 (2.3648)*	1.85

Table-4: Representing post buckling load (γ) of clamped orthotropic circular plates for the assumed function

$$F_3 = b_0\left[1+\alpha_1\left(\frac{r}{a}\right)^2+\alpha_2\left(\frac{r}{a}\right)^4\right]+b_1\left[\alpha_3\left(\frac{r}{a}\right)^2+\alpha_4\left(\frac{r}{a}\right)^4+\left(\frac{r}{a}\right)^6\right]+b_2\left[\alpha_5\left(\frac{r}{a}\right)^4+\alpha_6\left(\frac{r}{a}\right)^6+\left(\frac{r}{a}\right)^8\right]$$. '*' indicates the reference values taken from [3].

b_0/h	Present results									
	β = 1.2	Error (%)	β = 1.4	Error (%)	β = 1.6	Error (%)	β = 1.8	Error (%)	β = 2.0	Error (%)
0.0	2.2485 (2.1951)*	2.43	2.2386 (2.1924)*	2.11	2.2285 (2.1894)*	1.79	2.2197 (2.1860)*	1.54	2.2075 (2.1824)*	1.15
0.2	2.2745 (2.2031)*	3.24	2.2647 (2.2003)*	2.93	2.2534 (2.1972)*	2.56	2.2419 (2.1936)*	2.20	2.2258 (2.1899)*	1.64
0.4	2.3087 (2.2271)*	3.67	2.2963 (2.2239)*	3.26	2.2834 (2.2204)*	2.84	2.2729 (2.2164)*	2.55	2.2581 (2.2122)*	2.08
0.6	2.3461 (2.2666)*	3.50	2.3354 (2.2629)*	3.21	2.3221 (2.2587)*	2.81	2.3086 (2.2540)*	2.42	2.2921 (2.2491)*	1.91
0.8	2.3982 (2.3212)*	3.32	2.3846 (2.3167)*	2.93	2.3712 (2.3117)*	2.57	2.3582 (2.3061)*	2.26	2.3387 (2.3002)*	1.68
1.0	2.2616 (2.3902)*	2.99	2.4487 (2.3848)*	2.68	2.4362 (2.3788)*	2.41	2.4171 (2.3720)*	1.90	2.3986 (2.3648)*	1.43

The values of γ against various b_0/h for the assumed functions F_1, F_2 and F_3 with simply supported and clamped boundary conditions at β = 2.0 are illustrated in Fig. 2 and Fig. 3 respectively. From both graphs, it is clear that, the numerical results follow the same trend for all the admissible functions. Similarly, the other graphs for simply supported and clamped boundary conditions at different values of β also follow the same trend.

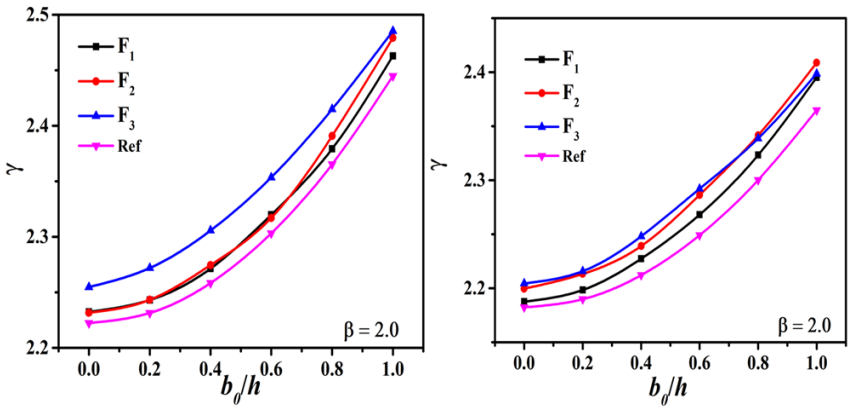

Fig-2: Comparison of postbuckling strength of simply supported and clamped orthotropic circular plates with known literature values at β = 2. Ref denotes the reference values taken from [33].

The problem stated in the paper is solved earlier using mathematical analysis like shooting method, finite element method, iterative method etc. But the complexity of the above mentioned mathematical methods prompted us to select a new numerical substitution method through which post-buckling load carrying capacity can be calculated. The present mathematical analysis helps in reducing the mathematical complexity and improving the accuracy of the result obtained.

CONCLUSIONS

A new mathematical approach to predict the thermal post-buckling behavior of orthotropic circular plates with simply supported and clamped boundary conditions are presented. The radial edge tensile load is evaluated by taking assumed functions for the lateral displacement and by introducing stress-free simplifications. The linear buckling load is evaluated by solving total potential energy equation based on von Kàrmàn nonlinearities. Hence the thermal

postbuckling load is calculated for various values of orthotropic parameter by using radial edge load and linear buckling load. The numerical results obtained from the present formulation show a satisfactory agreement with the previous results within the engineering accuracy. It gives a maximum error percentage of 4.02% for simply supported and 3.67% for clamped boundary conditions respectively. Moreover, the numerical results depend on the assumed functions which have taken and one should be cautious in selecting the functions to obtain reliable results.

ACKNOWLEDGEMENT

The authors would like to thank the Universiti Malaysia Pahang and Ministry of Higher Education, Malaysia for the provision in terms of financial form from the research grants (RDU160330 & PGRS170315).

REFERENCES

1. Thompson, J.M.T. & Hunt, G.W. (1973) . A general theory of elastic stability. J. Wiley.
2. Dym, C.L. (1974). Stability theory and its applications to structural mechanics. Springer Netherlands.
3. Kanaka Raju, K. & Rao, G. V, . Finite-element analysis of post-buckling behaviour of cylindrically orthotropic circular plates. Fibre Science and Technology, 19(2): p. 145-154.
4. Raju, K.K. & Rao, G.V. (1984). *Thermal post-buckling of circular plates.* Computers & Structures, 18(6): p. 1179-1182.
5. Rao, G.V. & Varma, R.R., (2007). *Simple formulation to predict thermal postbuckling load of circular plates.* AIAA Journal, 45(7): p. 1784-1786.
6. Raju, K.K. & Rao, G.V. (1984). *Finite element analysis of thermal postbuckling of tapered columns.* Computers & structures, 19(4): p. 617-620.
7. Rao, G. V & Raju, K. K., (2003). *Thermal postbuckling of uniform columns on elastic foundation - intuitive solution.* Journal of Engineering Mechanics, 129(11): p. 1351-1354.
8. Ramaraju, R.V. & Gundabathula, V.R. (2009). *Reinvestigation of intuitive approach for thermal postbuckling of circular plates.* AIAA Journal, 47(10): p. 2493-2495.
9. Berger, H.M. (1954). *A new approach to the analysis of large deflections of plates.* California Institute of Technology.
10. Sun, Y. & Li, S. R. (2014). *Thermal post-buckling of functionally graded material circular plates subjected to transverse point-space constraints.* Journal of Thermal Stresses, 37(10): p. 1153-1172.
11. Ma, L.S. & Wang, T.J. (2003). *Nonlinear bending and post-buckling of a functionally graded circular plate under mechanical and thermal loadings.* International Journal of Solids and Structures, 40(13–14): p. 3311-3330.
12. Ma, L. S. & Wang, T.J. (2003). *Axisymmetric post-buckling of a functionally graded circular plate subjected to uniformly distributed radial compression*. *Materials Science Forum*. (423-425): p. 719-724.
13. Najafizadeh, M. & Eslami, M. (2002). *First-order-theory-based thermoelastic stability of functionally graded material circular plates.* AIAA journal, 40(7): p. 1444-1450.
14. Najafizadeh, M.M. & Eslami, M.R. (2002). *Buckling analysis of circular plates of functionally graded materials under uniform radial compression.* International Journal of Mechanical Sciences, 44(12): p. 2479-2493.
15. Li, S.R., Batra, R.C., & Ma, L.S. (2007). *Vibration of thermally post-buckled orthotropic circular plates.* Journal of Thermal Stresses, 30(1): p. 43-57.
16. Raju, K.K. & Rao, G.V. (1996). *Thermal post-buckling of linearly tapered moderately thick isotropic circular plates.* Computers & Structures, 58(3): p. 655-658.
17. Rao, G. V, Reddy, G. K., Varma, R.R., & Rao, V. V. S. (2012). *Solution for large amplitude vibrations of circular plates via modified Berger's approximation.* The IES Journal Part A: Civil & Structural Engineering, 5(1): p. 56-61.
18. Raju, K.K. & Rao, G.V. (1985). *Post-buckling of cylindrically orthotropic linearly tapered circular plates by finite element method*. Computers & Structures, 21(5): p. 969-972.
19. Raju, K.K. & Rao, G.V. (1984). *Post-buckling of cylindrically orthotropic circular plates on elastic foundation with edges elastically restrained against rotation.* Computers & structures, 18(6): p. 1183-1187.
20. Raju, K.K. & Rao, G.V. (1988). *Post-buckling analysis of moderately thick cylindrically orthotropic circular plates.* Computers & structures, 29(4): p. 725-727.
21. Berger, H.M. (1955). *A new approach to the analysis of large deflections of plates.* journal of applied mechanics, 22: p. 465.
22. Bloom, F. & Coffin, D. (2000). *Handbook of thin plate buckling and postbuckling*. CRC Press.
23. Naidu, N.R., Raju, K.K. & Rao, G.V. (1993). *Post-buckling behaviour of circular plates resting on an axi-symmetric elastic partial foundation under uniform compressive loads.* Computers & Structures, 46(1): p. 187-190.

24. Gupta, R.K., Gunda, J. B., Janardhan, G. R., & Rao, G.V. (2010). *Thermal post-buckling analysis of slender columns using the concept of coupled displacement field.* International Journal of Mechanical Sciences, 52(4): p. 590-594.
25. Gupta, R.K., Gunda, J. B., Janardhan, G. R., & Rao, G.V. (2009). *Comparative study of thermal post-buckling analysis of uniform slender & shear flexible columns using rigorous finite element and intuitive formulations.* International Journal of Mechanical Sciences, 51(3): p. 204-212.
26. Gupta, R.K., Gunda, J. B., Janardhan, G. R., & Rao, G.V. (2010). *Post-buckling analysis of composite beams: Simple and accurate closed-form expressions.* Composite Structures, 92(8): p. 1947-1956.
27. Yamaki, N., (1961). *Influence of large amplitudes on flexural vibrations of elastic plates*. ZAMM - Journal of Applied Mathematics and Mechanics/Zeitschrift für Angewandte Mathematik und Mechanik, 41(12): p. 501-510.
28. Varma, R.R. & Rao, G.V. (2011). *Novel formulation to study thermal postbuckling of circular plates with edges elastically restrained against rotation.* Journal of Engineering Mechanics, 137(10): p. 708-711.
29. Nair, A.V., Kasim, A.R.M. & Salleh, M.Z. (2017). *A suitable numerical approximation for the thermal postbuckling behaviour of orthotropic circular plates*. *Journal of Physics: IOP Conference Series*.(890), 021061.